Electronic Supplementary Material (ESI) for Photochemical & Photobiological Sciences.

Supplementary Information

Metal-binding hydrazone photoswitches for visible light reactivity and variable relaxation kinetics

Kacey C. Hall, Andrew T. Franks, Rory C. McAtee, Michael S. Wang, Vivian I. Lu, and Katherine J. Franz[a] *

[a] Department of Chemistry
Duke University
Durham, NC
27708 USA
katherine.franz@duke.edu

Table of Contents

1. Synthesis of HAPI and Derivatives ---------- S3–S4
2. UV-vis spectra of Ground State and Photostationary States in DMSO ---------- S5-S6
3. Beer's Plots of HAPI and Derivatives ---------- S7–S8
4. HAPI Spectra in Different Solvents and pH ---------- S9
5. ^{1}H NMR shifts for hydrazone phenolic (O-H) and amide (N-H) protons in d_6-DMSO ---------- S10
6. Emission Spectra of Light Sources ---------- S11
7. Actinometry of Light Sources ---------- S12
8. Reversibility/ Thermal Relaxation Kinetics (*Z*→*E*) in DMSO After UVA Irradiation ----- S13–S15
9. Thermal Relaxation in MeCN After UVA Irradiation ---------- S16–S17
10. LC-MS of Initial and UVA/UVC PSS, calculating %conversion ---------- S18–S25
11. Calculation of Extinction Coefficients for *E* and *Z* isomers for HAPI & Derivatives ------ S26–S27
12. Calculations for Composition of Blue Light Treatment ---------- S27
13. HAPI Thermal Relaxation Rates in Different Solvents ---------- S28–S29
14. Effect of sampling time of UV-VIS on HAPI isomer equilibrium ---------- S29
15. Assessment of Iron(III) Affinity ---------- S30

1. Synthesis of HAPI and Derivatives

(*E*)-N'-(1-(2-hydroxyphenyl)ethylidene)isonicotinohydrazide **(HAPI)** and hydrazones **1, 6**, **7**, **9**, **10 (94% yield)**, and **13 (91% yield)** (see **Figure 1** for structures) were prepared according to the literature procedure for condensation of aroylhydrazides and acetophenones. Identity and purity were confirmed by ^{1}H NMR and LC-HRMS. Isonicotinic acid hydrazide (Acros Organics), 2-hydroxy-trifluoroacetophenone (Oakwood Chemical), 2-acetyl-1-naphthol (Acros Organics), 2',5'-dihydroxyacetophenone (Alfa Aesar), 4-dimethylaminobenzoic hydrazide (Alfa Aesar), and 2',4'-dihydroxyacetophenone (Ark Pharm, Inc.) were purchased in reagent grade and used without further purification. All other reagents were purchased from Sigma Aldrich Corp. ^{1}H NMR spectroscopy was performed on a Varian 400 MHz spectrometer. Exact mass measurements were acquired using an Agilent 6224 TOF-ESI-MS.

(*E*)-N'-(2,2,2-trifluoro-1-(2-hydroxyphenyl)ethylidene)isonicotinohydrazide (2): 2-hydroxy-trifluoroacetophenone (163 mg, 0/857 mmol) and isonicotinic acid hydrazide (117 mg, 0.857 mmol) were added to absolute ethanol (5 mL). The mixture was heated to reflux. After cooling, the solvent was removed and the remaining residue was purified by silica column chromatography (100% ethyl acetate eluent) to yield an off-white solid (0.09g, 0.29 mmol, 34% yield). ^{1}H NMR (400 MHz, d_6-DMSO) δ 11.28 (s, 1H), 10.40 (s, 1H), 8.72 (s, 2H), 7.57 (d, J = 4.4 Hz, 2H), 7.39 (t, J = 7.5 Hz, 1H), 7.24 (d, J = 7.4 Hz, 1H), 7.00 (d, J = 8.2 Hz, 2H), 6.94 (t, J = 7.3 Hz, 1H). HR-ESIMS (m/z): calcd for $[M + H]^+$ $C_{14}H_{10}F_3N_3O_2$ is 310.0798, found 310.0803.

(*E*)-N'-(1-(2-hydroxyphenyl)ethylidene)benzohydrazide (3): Portions of 2'-hydroxyacetophenone (0.50 mL, 4.4 mmol) and benzhydrazide (0.59 g, 4.4 mmol) were combined in absolute ethanol (25 mL) and acetic acid (2 mL) then stirred at reflux overnight. Upon cooling to room temperature, the resulting precipitate was collected by vacuum filtration, washed with 95% ethanol and dried in a vacuum oven to yield pale yellow crystals (446 mg, 40% yield) ^{1}H NMR (400 MHz, d_6-DMSO): δ ppm 13.36 (s, 1H), 11.34 (s, 1H), 7.94 (dd, J = 7, 1 Hz, 2H), 7.67-7.60 (m, 2H), 7.59-7.51 (m, 2H), 7.31 (ddd, J = 8, 8, 1 Hz, 1H), 6.95-6.88 (m, 2H), 2.49 (s, 3H) HR-ESIMS (m/z): calcd for $[M + H]^+$ $C_{15}H_{14}N_2O_2$ is 255.1128, found 255.1138

(*E*)-4-amino-N'-(1-(2-hydroxyphenyl)ethylidene)benzohydrazide (**4**): A portion of 2-hydroxyacetophenone (199 μL, 1.65 mmol) was added to a roundbottom flask and dissolved in 5 mL absolute ethanol. To the flask, 4-aminobenzoic hydrazide (250 mg, 1.65 mmol) and acetic acid (0.5 mL) were added. The mixture was stirred at reflux for 3 h; during this time the heterogeneous mixture dissolved completely before a precipitate formed. The reaction mixture was cooled to 0°C then filtered via vacuum filtration. The remaining solid was washed with chilled ethanol then dried in a vacuum oven to afford light yellow crystals (409 mg, 92% yield). ^{1}H NMR (400 MHz, d_6-DMSO) δ (ppm): 13.46 (s, 1H), 10.80 (s, 1H), 7.66 (d, J = 9 Hz, 2H), 7.57 (dd, J = 8, 2 Hz, 1H), 7.24 (ddd, J = 8, 7, 2 Hz, 1H), 6.86 (d, J = 8 Hz, 1H), 6.84 (ddd, J = 9 Hz, 7 Hz, 1 Hz, 1H), 5.81 (s, 2H), 2.42 (s, 3H) HR-ESIMS (m/z): calcd for $[M + H]^+$ $C_{15}H_{15}F_3N_3O_2$ is 270.1237, found 270.1235

(*E*)-N'-(1-(2-hydroxyphenyl)ethylidene)-4-nitrobenzohydrazide (**5**): 2-hydroxyacetophenone (0.190 mL, 1.83 mmol) and 4-nitrobenzoic hydrazide (0.331 g, 1.83 mmol) were combined in a flask with ethanol (10 mL) and acetic acid (1.0 mL). The mixture was heated to reflux overnight. After cooling on ice, the precipitate was isolated by vacuum filtration and washed with cold EtOH. Solid **5** was dried in a vacuum oven to give yellow crystals (544 mg, 99% yield). ^{1}H NMR (400 MHz, d_6-DMSO) δ (ppm): 13.22 (s, 1H) 11.63 (s, 1H), 8.35 (d, J = 8 Hz, 2H), 8.16 (d, J = 8 Hz, 2H), 7.63 (d, J = 8 Hz, 1H), 7.30 (dd, J = 8, 8 Hz, 1H), 6.91-6.87 (mult, 2H) 2.49 (s, 3H) HR-ESIMS (m/z): calcd for $[M + H]^+$ $C_{15}H_{13}N_3O_4$ is 300.0979, found 300.0966

(*E*)-N'-(1-(4-fluoro-2-hydroxyphenyl)ethylidene)isonicotinohydrazide (**8**): 4'-fluoro-2'-hydroxyacetophenone (0.44 g, 3.23 mmol) and isonicotinic acid hydrazide (0.50 g, 3.23 mmol) were dissolved in 10 mL absolute ethanol and 1 mL acetic acid. The mixture was refluxed overnight and a precipitate formed. Upon cooling to room temperature, the precipitate was filtered A white crystalline powder was collected by vacuum filtration with no further purification (577 mg, 74% yield). ^{1}H NMR (d_6-DMSO, 400 MHz) δ (ppm): 13.71 (s, 1H), 11.62 (s, 1H), 8.82 (d, J = 6 Hz, 2H), 7.84 (d, J = 6 Hz, 2H), 7.74-7.70 (m, 2H) 6.80-6.70 (m 2H), 2.47 (s, 3H) HR-ESIMS (m/z): calcd for $[M + H]^+$ $C_{14}H_{12}FN_3O_2$ is 274.0986, found 274.0984

(*E*)-N'-(1-(2,5-dihydroxyphenyl)ethylidene)isonicotinohydrazide (**11**): Isonicotinic acid hydrazide (0.45 g, 3.28 mmol) and 2',5'-dihydroxyacetophone (0.50 g, 3.28 mmol) were combined in a roundbottom flask with 25 mL ethanol and 2 mL acetic acid. The solution was heated to reflux and stirred overnight. Upon cooling, the resulting precipitate was filtered, washed with ethanol, then dried in a vacuum oven to produce a yellow powder (891 mg, 76% yield). ^{1}H NMR (d_6-DMSO, 400 MHz) δ (ppm) 12.41 (s, 1H), 11.51 (s, 1H), 8.93 (s, 1H), 8.77 (d, J = 6 Hz, 2H), 7.82 (d, J = 6 Hz, 2H), 6.97 (d, J = 3 Hz, 1H), 6.76 (dd, J = 9, 3 Hz, 1H), 6.72 (d, J = 9 Hz, 1H), 2.40 (s, 3H) HR-ESIMS (m/z): calcd for $[M + H]^+$ $C_{14}H_{13}N_3O_3$ is 272.1030, found 272.1024

(*E*)-N'-(1-(2-hydroxy-5-methoxyphenyl)ethylidene)isonicotinohydrazide (**12**): Portions of isonicotinic acid hydrazide (825 mg, 6.02 mmol) and 2'-hydroxy-5'-methoxyacetophenone (999 mg, 6.02 mmol) were combined in a 100-mL roundbottom flask with 50 mL absolute ethanol and 3 drops glacial acetic acid. The mixture was heated to reflux overnight then cooled to room temperature. The solid product was isolated by vacuum filtration, rinsed with H_2O and chilled ethanol, and dried to give a yellow powder (850 mg, 50% yield). ^{1}H NMR (d_6-DMSO, 400 MHz) δ (ppm) 12.66 (s, 1H), 11.57 (s, 1H), 8.80 (d, J = 6 Hz, 2H), 7.85 (d, J = 6 Hz, 2H), 7.15 (d, J = 3 Hz, 1H), 6.97 (dd, J = 9, 3 Hz, 1H), 6.87 (d, J = 9 Hz, 1H), 3.76 (s, 3H), 2.52 (s, 3H) HR-ESIMS (m/z): calcd for $[M + H]^+$ $C_{15}H_{15}N_3O_3$ is 286.1186, found 286.1189

(*E*)-N'-(1-(2-hydroxyphenyl)ethylidene)-3,4,5-trimethoxybenzohydrazide (**14**): Compound **14** was synthesized from 2'-hydroxyacetophenone (250 mg, 1.83 mmol) and 3,4,5-trimethoxybenzoic acid hydrazide (414 mg, 1.83 mmol) following the procedure used for **4** to yield white crystals (442 mg, 70% yield). ^{1}H NMR (d_6-DMSO, 400 MHz) δ (ppm): 13.34 (s, 1H), 11.23 (s, 1H), 7.65 (d, J = 8 Hz, 1H), 7.32 (dd, J = 8, 8 Hz, 1 H), 7.25 (s, 2H), 6.94-6.89 (mult, 2H), 3.88 (s, 6H), 3.74 (s, 1H), 2.50 (s, 3H) HR-ESIMS (m/z): calcd for $[M + H]^+$ $C_{18}H_{20}N_2O_5$ is 345.1445, found 345.1446

(*E*)-N'-(1-(2-methoxyphenyl)ethylidene)isonicotinohydrazide (**15**): A portion of 2'-methoxyacetophenone (284 mg, 1.89 mmol) was dissolved in absolute ethanol (10 mL). Isonicotinoyl hydrazide (259 mg, 1.89 mmol) was added to the solution, followed by addition of 2 drops of glacial acetic acid. Approximately 1 g $MgSO_4$ was added to the reaction flask. The heterogeneous mixture was heated to reflux overnight then vacuum filtered while still warm to remove $MgSO_4$. The filter paper was rinsed with methanol. Upon standing, the filtrate produced a white crystalline solid out of a yellow solution. The supernatant was removed by filtration and the crystals were washed with cold methanol. Product was recrystallized from hot methanol (106 mg, 21% yield). ^{1}H NMR (d_6-DMSO, 400 MHz) δ (ppm): 10.91 (s, 1H), 8.76 (d, J = 5 Hz, 2H), 7.79 (d, 5 Hz, 2H), 7.41 (dd, J = 8, 7 Hz, 1H), 7.33 (d, J = 7 Hz), 7.11 (d, J = 8 Hz, 1H), 7.00 (dd, J = 8, 7 Hz, 1H), 3.83 (s, 3H), 2.30 (s, 3H) HR-ESIMS (m/z): calcd for $[M + H]^+$ $C_{15}H_{15}N_3O_2$ is 270.1244, found 270.1237

(*E*)-N'-(1-(1-hydroxynaphthalen-2-yl)ethylidene)isonicotinohydrazide (**16**): 2-acetyl-1naphthol (0.68 g, 3.65 mmol) and isonicotinic acid hydrazide (0.50 g, 3.65 mmol) were dissolved in 10 mL 1-propanol and 1 mL acetic acid. The mixture was refluxed overnight and a precipitate formed. Upon cooling to room temperature, the precipitate was filtered. An orange powder was collected by vacuum filtration with no further purification (758 mg, 68% yield). ^{1}H NMR (400 MHz, d_6-DMSO) δ 14.82 (s, 0H), 11.69 (s, 0H), 8.82 (d, J = 4.2 Hz, 1H), 8.35 (d, J = 8.2 Hz, 1H), 7.87 (t, J = 5.9 Hz, 2H), 7.74 (d, J = 8.7 Hz, 1H), 7.56 (dt, J = 21.4, 6.9 Hz, 1H), 7.41 (s, 1H), 2.61 (s, 1H).

2. UV-vis Spectra of Ground State and Photostationary States in DMSO

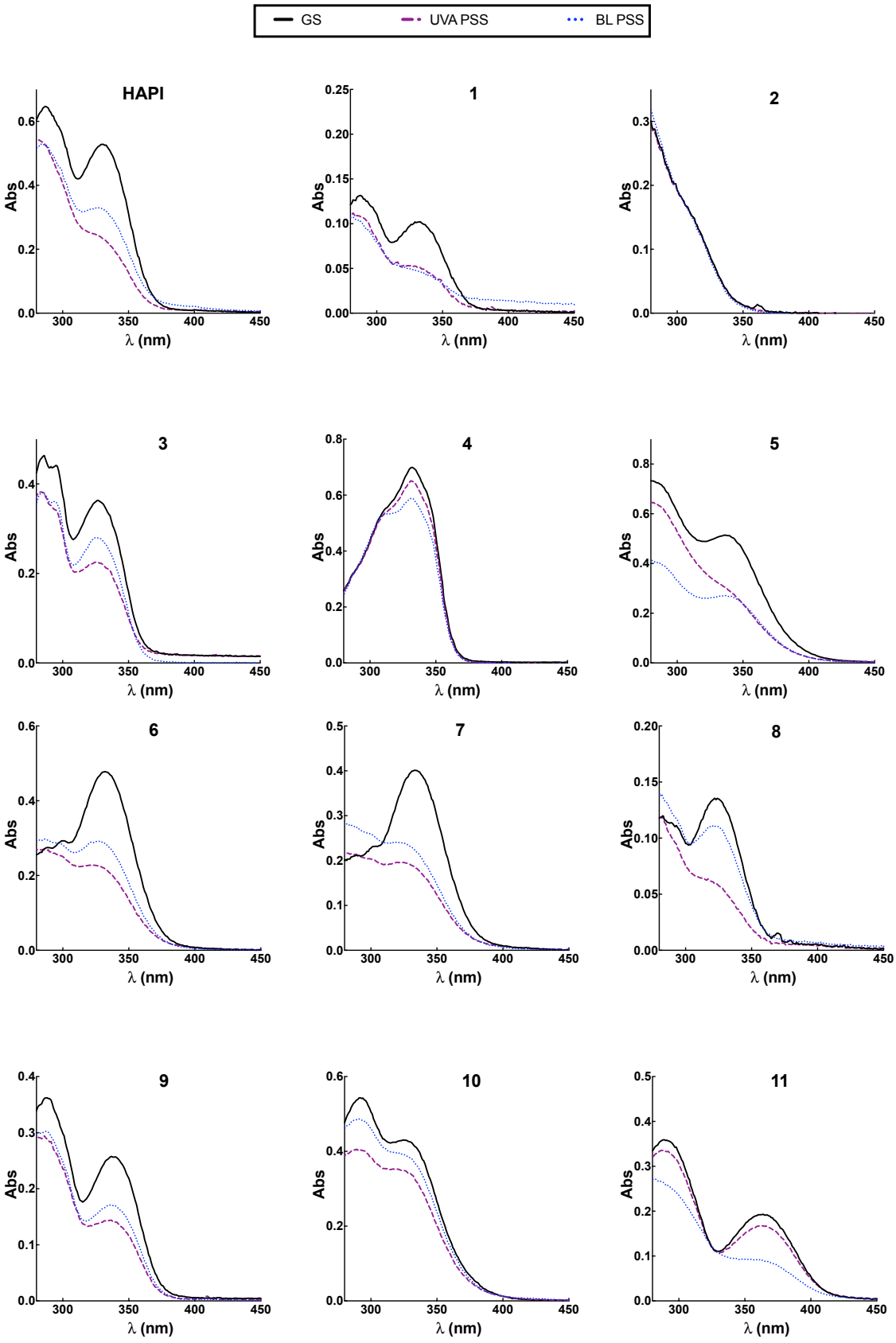

Figure S1, cont.

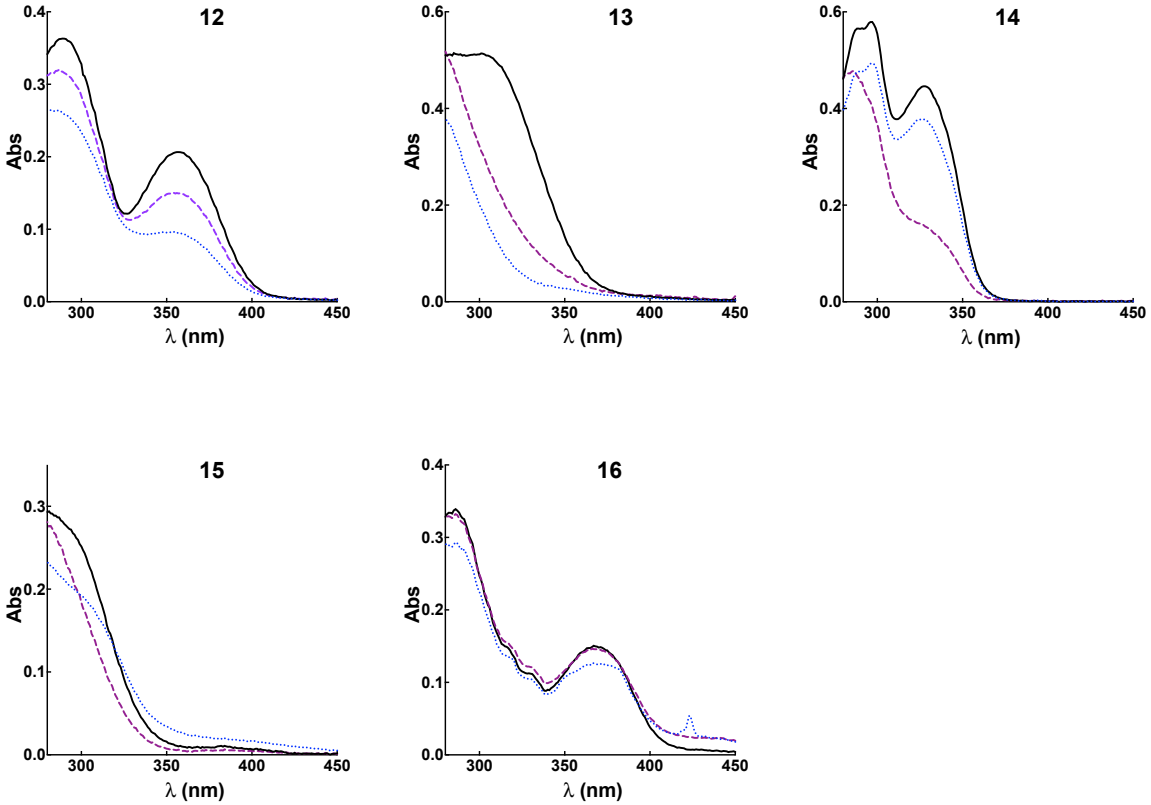

Figure S1. Response to different light sources. Irradiation of aroylhydrazone chelators alters UV-visible absorption. Solutions of aroylhydrazones in DMSO exhibit diverse absorption profiles (solid black line). Samples were irradiated until the spectra no longer changed either with broadband UVA light (dash purple line) or blue light (dotted blue line). The equilibrium between the two isomers is shifted by the different light sources as can be seen by the different absorption profiles. Most solutions were 25 μM in compound, except HAPI (50 μM), **1** (10 μM), **2** (30 μM), **8** (10 μM), and **16** (10 μM). **Instrument settings:** Ave time – 0.0125 s; Data Interval – 1.00 nm; Scan Rate – 4800.00 nm/min; Scan width – 800 to 200 nm.

3. Beer's Plot of HAPI and Derivatives

Beer's plot for each derivative were completed for both the ground state and irradiated state to ensure further analysis on the compounds was in the linear range. Serial dilutions of each compound was completed. For each derivative at each concentration, a UV-vis spectra was taken before treatment. Each sample was irradiated with UVA light until the spectra no longer changed, and another UV-vis spectra was taken. Absorbance at a chosen wavelength was plotted against concentration to produce the Beer's plot.

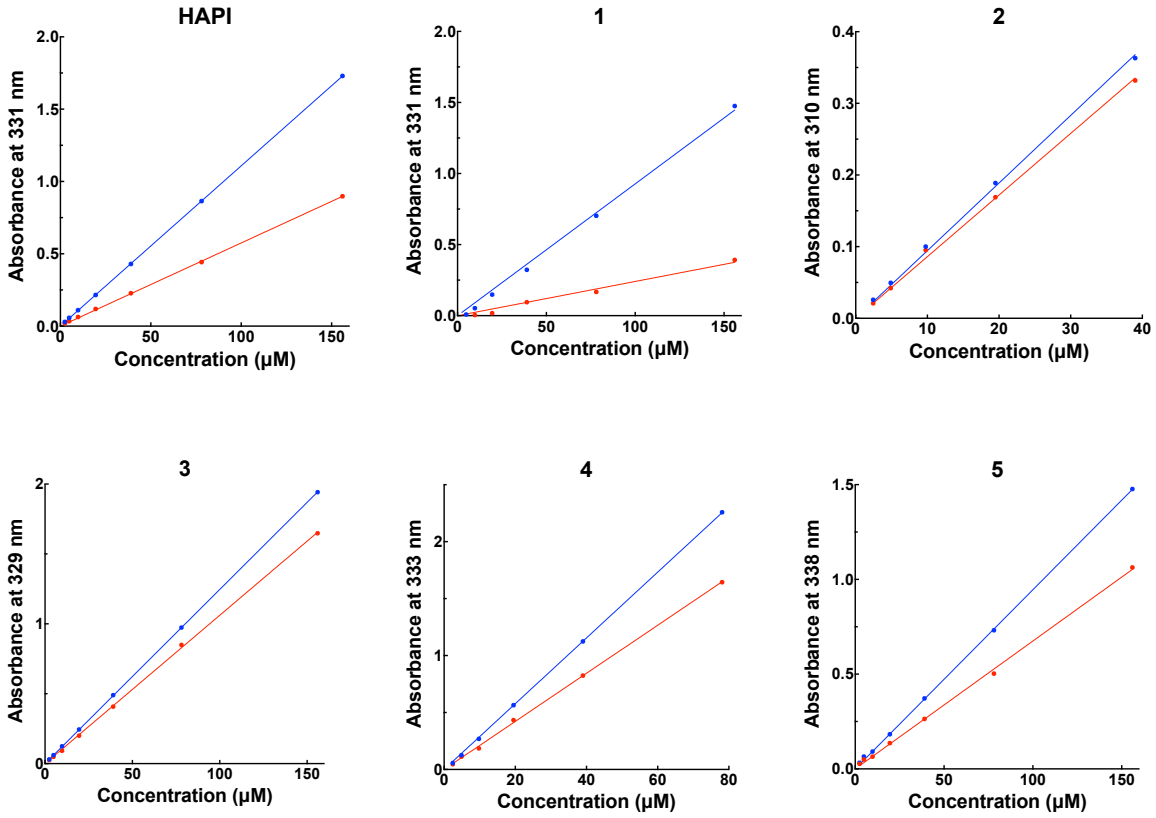

Figure S2. Beer's plot for HAPI and derivatives of absorption vs. concentration. A serial dilution of each compound was completed. The blue line represents the Beer's plot analysis for the ground state, and the red line represents the PSS. At each concentration, an absorbance spectrum was taken. Then, the sample was irradiated with UVA light until the PSS was reached, and another absorbance spectrum was taken. The absorbance at a λ_{max} for each compound was extracted from the full spectrum, and plotted against concentration. Only concentrations that fell in the linear range of the Beer's plot were used for further analysis. **Instrument settings:** Ave time – 0.0125 s; Data Interval – 1.00 nm; Scan Rate – 4800.00 nm/min; Scan width – 800 to 200 nm.

(cont. next page)

Figure S2, cont.

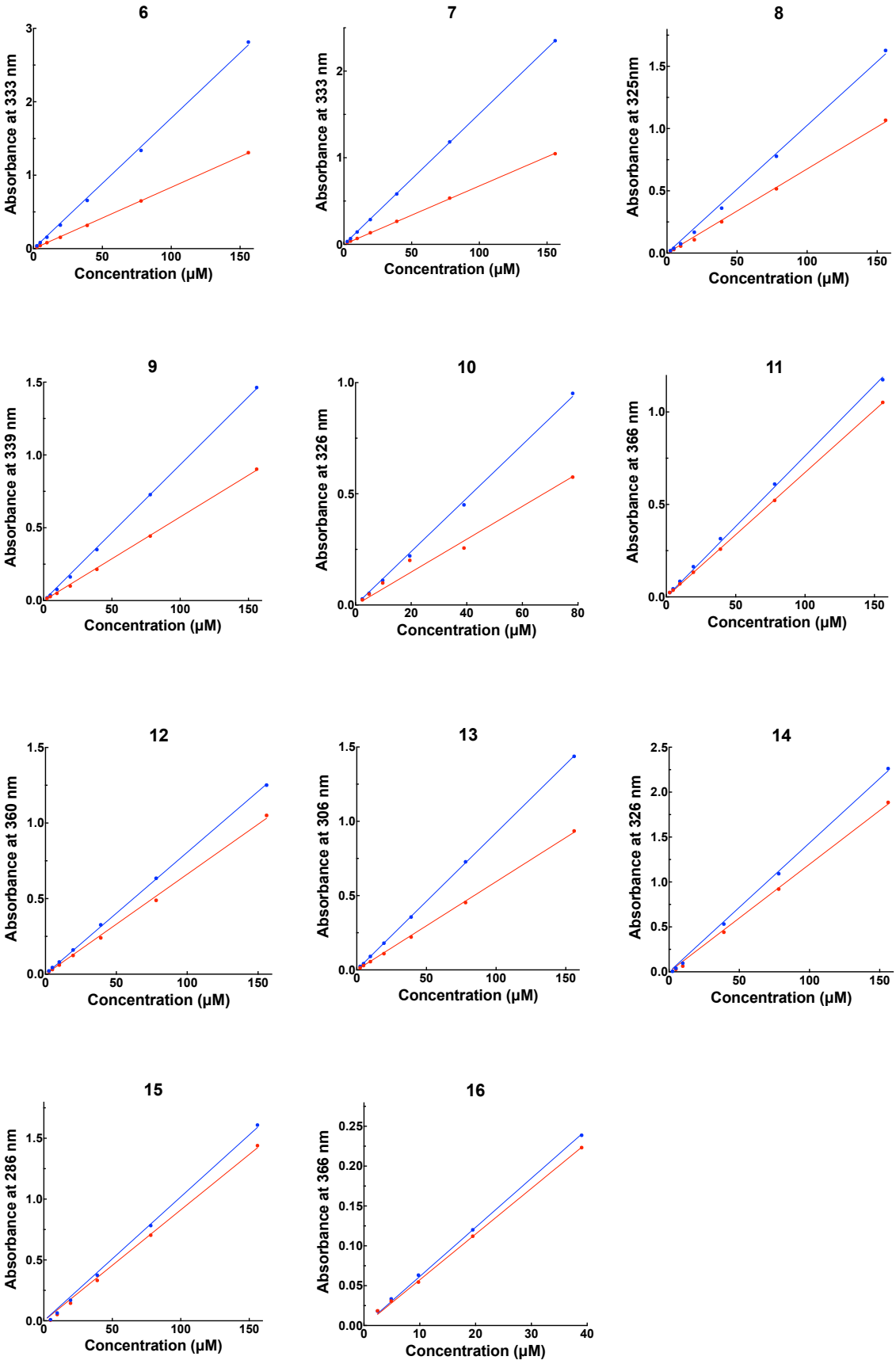

4. HAPI Spectra in Different Solvents and pH

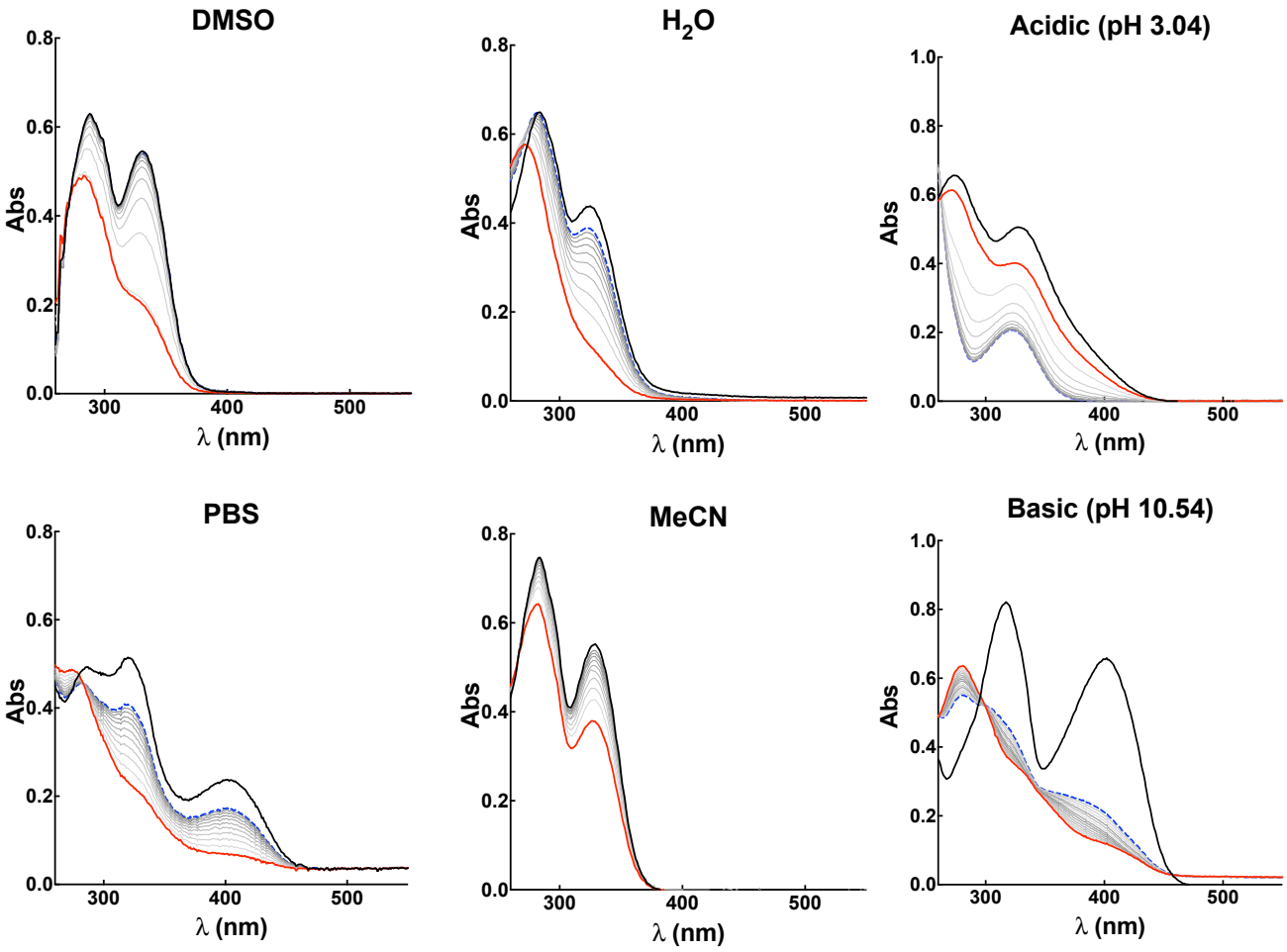

Figure S3. HAPI in different solvents. 50 µM solutions of HAPI were prepared in DMSO, DI H_2O (pH ~5.9), PBS (Phosphate Buffered Saline, pH 7.4), MeCN, Acidic pH, and Basic pH (solid black line). Samples were irradiated with broadband UVA light (red line). A UV-Vis scan was taken every hour (solid gray lines) for 10 h (blue dashed line). **Instrument settings:** Ave time – 0.0125 s; Data Interval – 1.00 nm; Scan Rate – 4800.00 nm/min; Scan width – 800 to 200 nm.

5. ^{1}H NMR shifts for hydrazone phenolic (O-H) and amide (N-H) protons in d_6-DMSO

Table S1. NMR spectra were collected on a Varian 400 mHz instrument. The ^{1}H NMR spectra of the compounds often contain a strongly deshielded proton signal with a chemical shift $\delta \geq 12$ ppm. This peak has been previously attributed to the deshielding effect of the nearby ketimine nitrogen.

Compound	σ(O-H)	σ(N-H)
HAPI	13.21	11.59
1	13.27	11.61
2	11.25	10.39
3	13.37	11.33
4	13.48	10.82
5	13.29	11.65
6	13.60	11.48
7	13.40	11.41
8	13.74	11.63
9	13.29	11.67
10	14.41	11.86
11	12.53	11.53
12	12.70	11.57
13	11.41	11.08
14	13.34	11.23
15	N/A	10.91
16	14.82	11.69

6. Emission Spectra of Light Sources

The UVA and UVC light sources consisted of eight light bulbs with emission centered at 371 or 254 nm, respectively, in a carousel photoreactor that situated the samples approximately 11 cm from the light bulbs. The blue light source contained three Prolight 1-watt ultraviolet LED light bulbs with emission centered at 395 nm arranged approximately 3 cm around the sample.

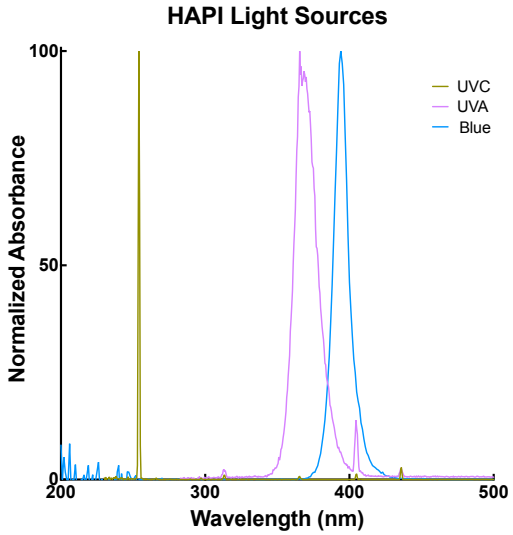

Figure S4. Emission Spectra of Light Sources Used in Experiments. Normalized emission spectra of each light source showing emission maxima at 371 ± 11 nm for UVA (purple line), 254 nm for UVC (yellow line), and 395 ± 5 nm for the blue light source (blue line). All spectra were collected using a FLSP920 spectrometer (Edinburg Instruments Ltd. Livingston, UK) and normalized to themselves, using the formula $(X - X_{min})/(X_{max}-X_{min})$.

7. Actinometry of Light Sources

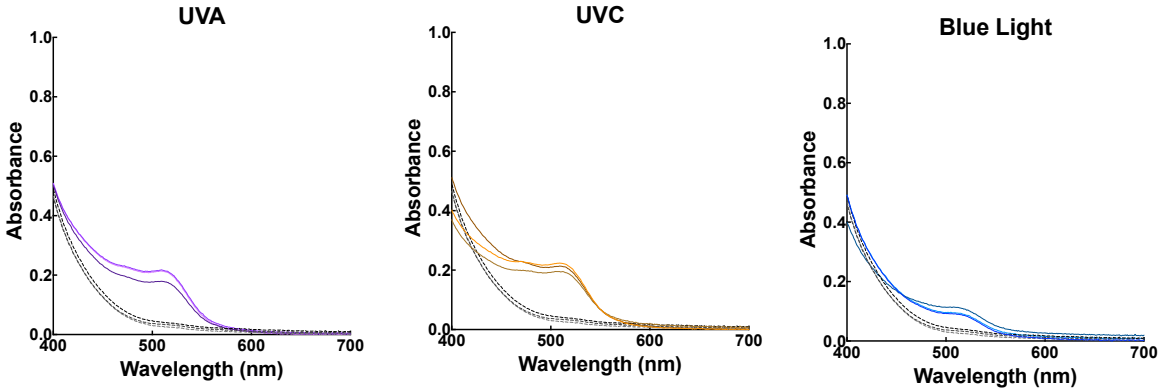

Figure S5. Absorption Spectra of Each Light Source for Ferrioxalate Actinometry. Solutions of ferrioxalate were irradiated with each light source. The light causes the decomplexation of the iron-oxalate complex, leaving free iron in solution. This irradiated solution is added to phenanthroline. The phenanthroline complexes with the free iron in solution, and this can be monitored spectroscopically at 510 nm by the formation of phenanthroline-iron charge transfer band. The reference treatment is shown as a black dotted line. The color traces represent the formation of the phenanthroline-iron complex.

Ferrioxalate actinometry was completed to characterize the light sources used. All procedures were used following IUPAC guidelines published by Kuhn et al.[1,2] All procedures were completed under red light. A 0.006 M solution of ferrioxalate was made by dissolving iron (III) potassium oxalate trihydrate (2.947 g) in 100 mL H_2SO_4 (0.5 M) and diluted to 1000 mL with DI water in a volumetric flask. A 0.1% 1,10-phenathroline solution was prepared by dissolving 1,10-phenanthroline monohydrate (0.5g) in 500 mL of DI water. Buffer solution was prepared by dissolving sodium propionate (82 g) in 10 mL conc. H_2SO_4, and diluted to 1000 mL in a volumetric flask.

3 mL (V_1) of the 0.006 M ferrioxalate solution was irradiated by each light source for exactly 15 sec (5 sec for UVA light) while effectively stirring. 1 mL (V_2) of the irradiated solution was added to a 10 mL (V_3) volumetric flask. 4 mL of the phenanthroline solution to the volumetric flask and diluted to 10 mL with DI water. A reference solution was made in the same manner, except the ferrioxalate solution was not irradiated. After 1 h, an absorption spectrum was taken of both the reference and irradiated samples. Each sample was run in triplicate. The photon flux ($q_{n,p}$ in Einstein/s) was calculated using the following equation:

$$q_{n,p} = \frac{\Delta A \, V_1 V_3}{\Phi(\lambda) \, \varepsilon(510\ nm) \, V_2 l \, t}$$

where ΔA is the difference in absorbance at 510 nm of the reference cell and irradiated sample, l is the optical pathlength, t is the time of total irradiation in seconds, $\Phi(\lambda)$ is the quantum yield of the ferrioxalate-phenanthroline complex at the defined wavelength being used, and $\varepsilon(510\ nm)$ is the molar absorptivity of ferrioxalate-phenanthroline complex at the defined wavelength being used.

	Photon Flux ***(10^{-8} Einstein/s)***
UVA	7.5(9)
UVC	2.5(2)
BL	1.0(2)

8. Reversibility/Thermal Relaxation Kinetics (*Z*→*E*) in DMSO After UVA Irradiation

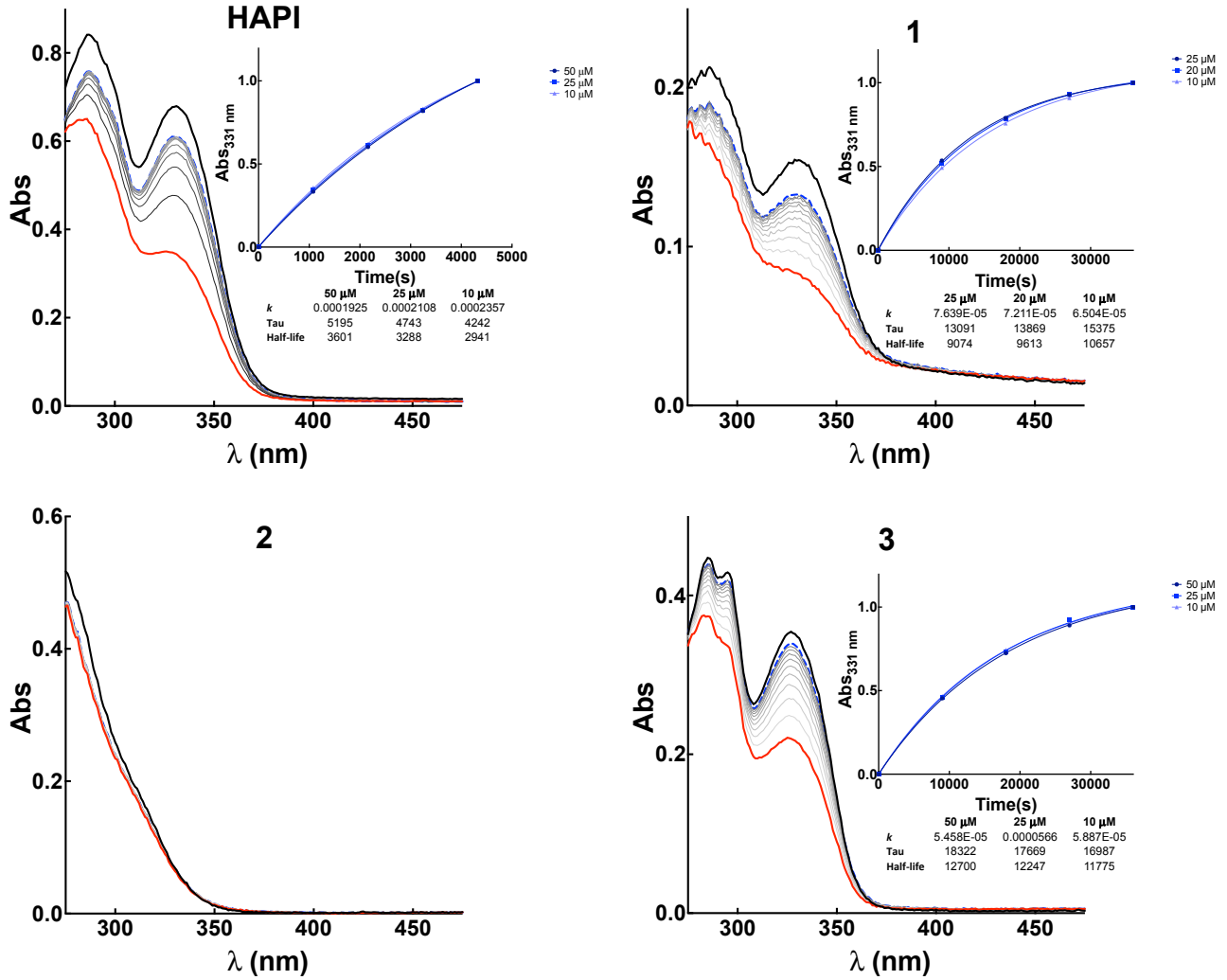

Figure S6. Thermal relaxation rates of HAPI and its derivatives after UVA irradiation to PSS. Fresh solutions of aroylhydrazones in DMSO were monitored by UV-Vis spectroscopy (solid black lines), and were irradiated with broadband UVA light (red lines). A UV-Vis scan was taken every hour (solid gray lines) for 10 hours (blue dashed line). Most compounds were run at 25 µM except HAPI (50 µM), Compound **1** (10 µM), Compound **2** (30 µM), Compound **8** (10 µM), and Compound **16** (10 µM). **Instrument settings:** Ave time – 0.0125 s; Data Interval – 1.00 nm; Scan Rate – 4800.00 nm/min; Scan width – 800 to 200 nm. **Inset:** For each compound, 3 concentrations were used to demonstrate an independence of the rate on concentration. Compound **2** and **16** do not react significantly to UVA light, so a rate was not determined. For each compound, at each concentration, the sample was irradiated with UVA light until the PSS was reached. Samples were monitored by UV-vis chosen for a specific wavelength. Time-points were taken every 2.5 hours over a 10-hour period for compounds with longer half-lives, or every 18 minutes over 72 minutes for compounds with shorter half-lives. Data for each compound was normalized ($X-X_{min}/X_{max}-X_{min}$) and a non-linear regression one-phase association fit using Prism graphing software was applied to give the rate (K) and half-life. **Instrument settings:** Ave time – 0.0125 s

(cont. next page)

Figure S6, cont.

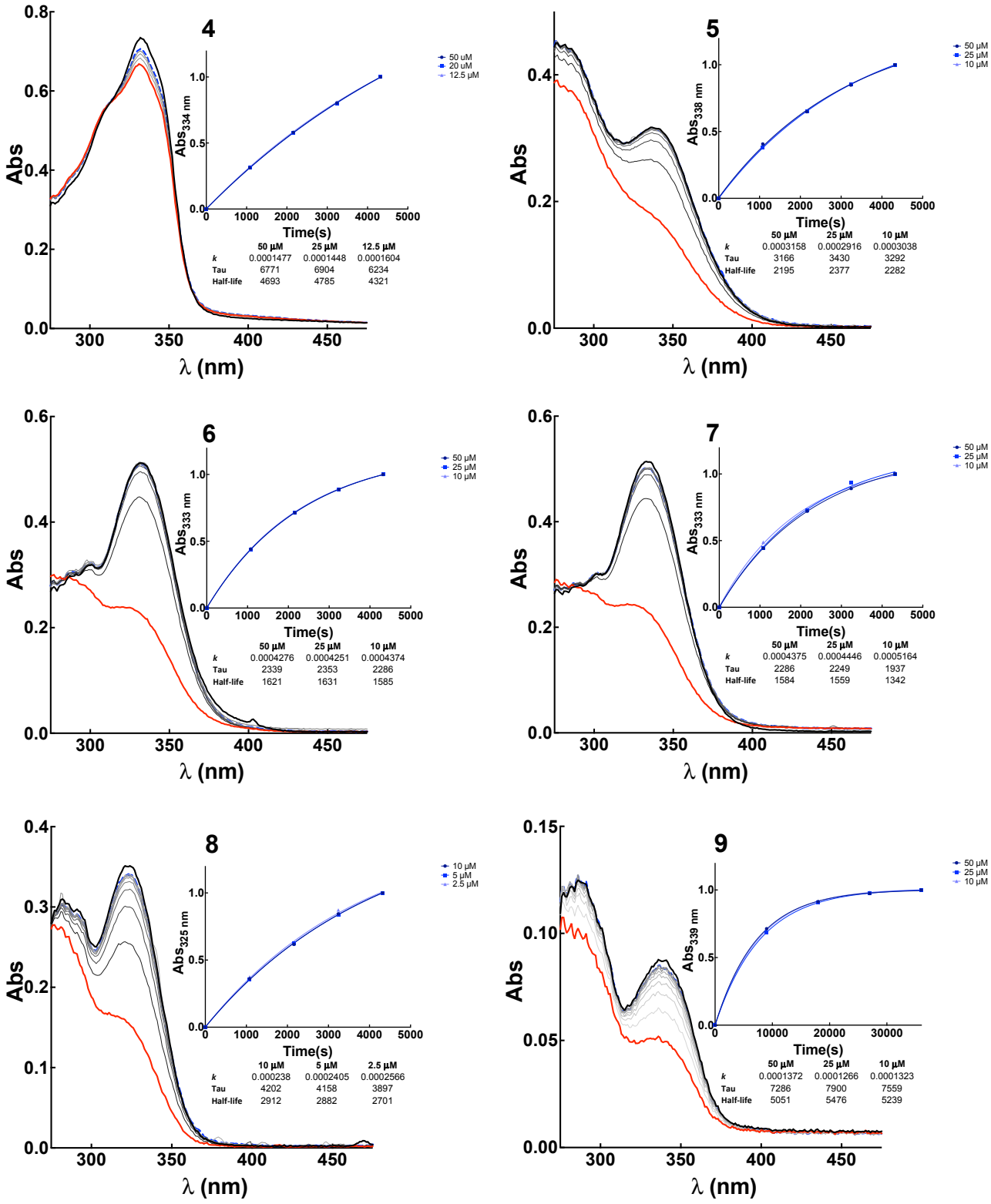

Figure S6, cont.

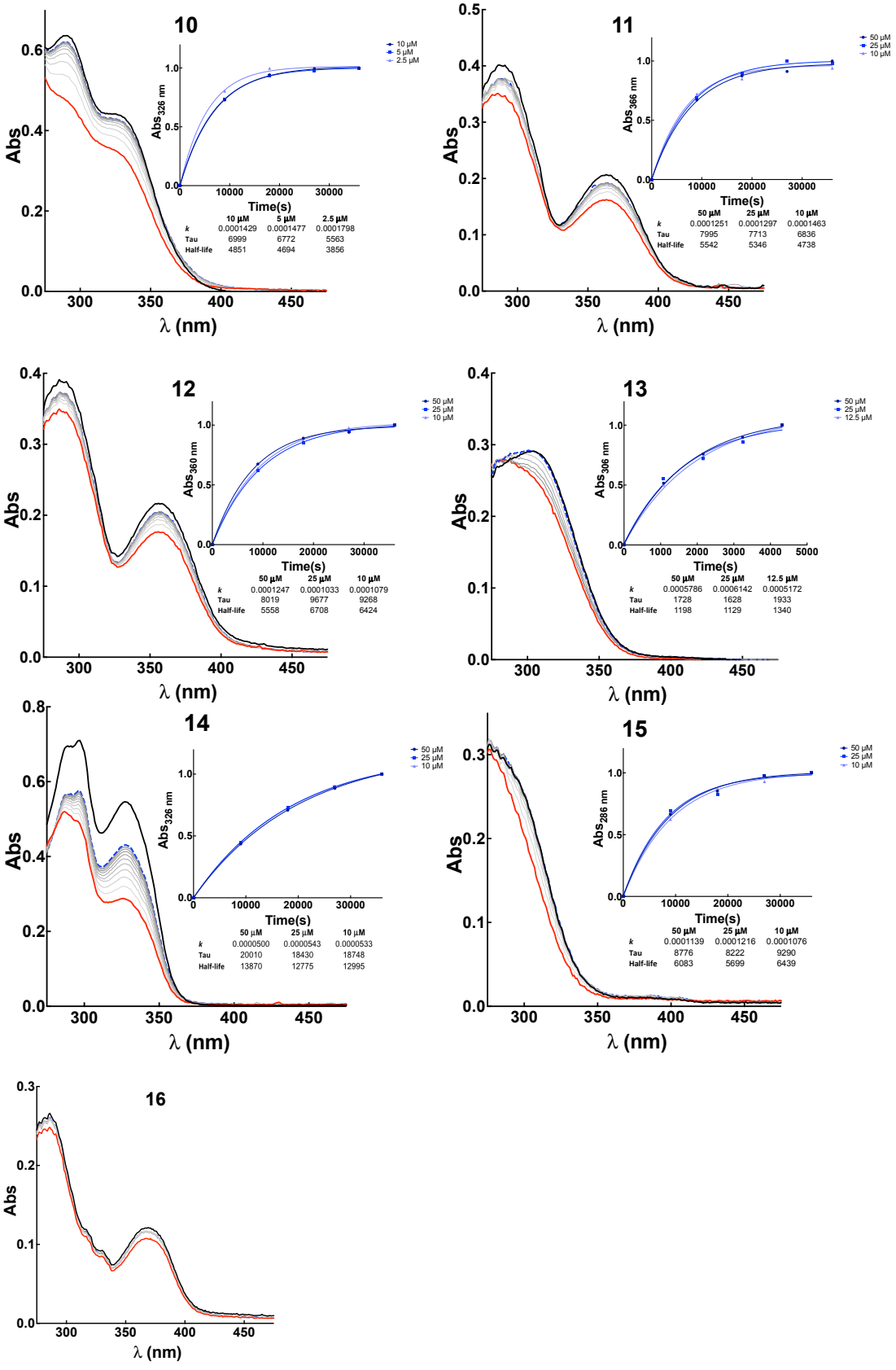

9. Thermal Relaxation in MeCN after UVA irradiation

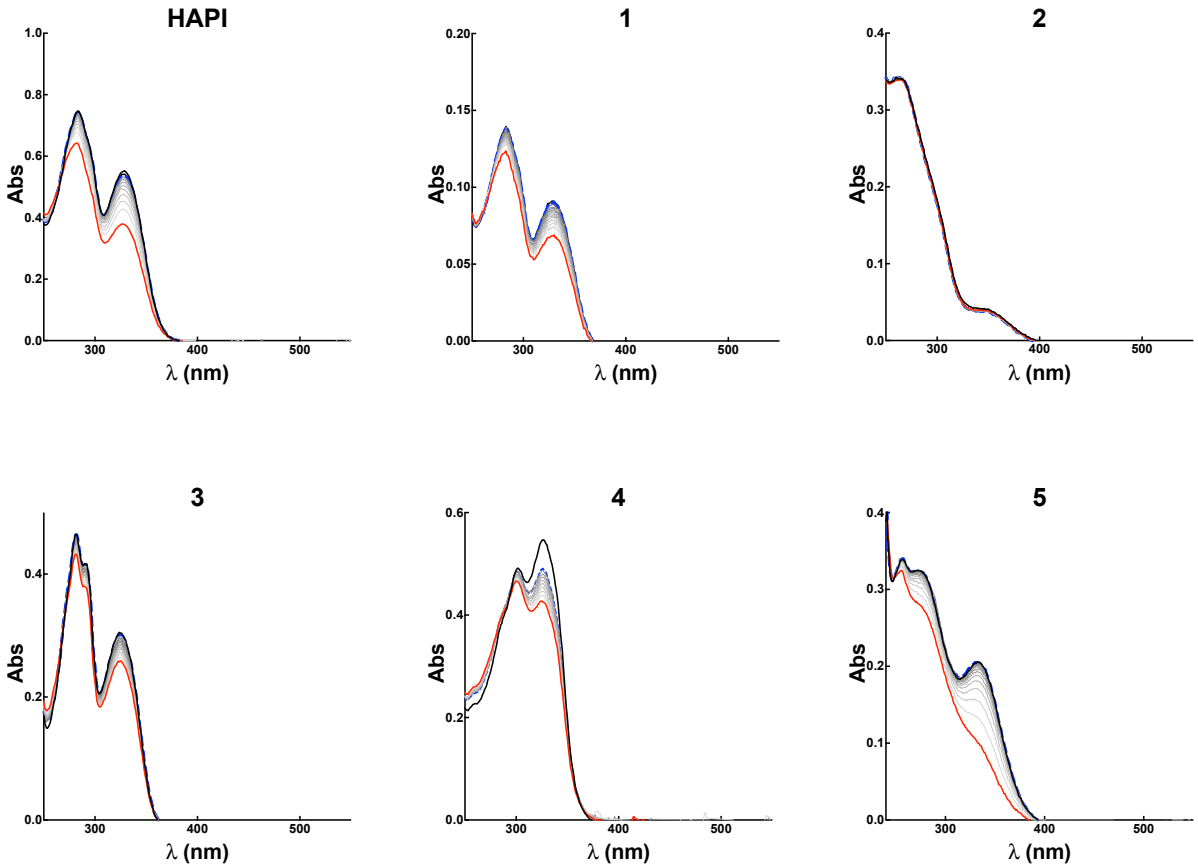

Figure S7. Thermal relaxation rates of HAPI and its derivatives after UVA irradiation to PSS, full spectrum in MeCN. Fresh solutions of aroylhydrazones in MeCN were monitored by UV-Vis spectroscopy (solid black lines), and were irradiated with broadband UVA light (red lines). A UV-Vis scan was taken every hour (solid gray lines) for 10 hours (blue dashed line). Most compounds were run at 25 μM except HAPI (50 μM), Compound **1** (10 μM), Compound **2** (30 μM), Compound **8** (10 μM), and Compound **16** (10 μM). This experiment was completed to show isosbestic points of each of the derivatives since these points are not obvious in DMSO. Isosbestic points are not obvious in DMSO because DMSO absorbs in the region where most of these points occur. **Instrument settings:** Ave time – 0.0125 s; Data Interval – 1.00 nm; Scan Rate – 4800.00 nm/min; Scan width – 800 to 200 nm.

(cont. on next page)

Figure S7, cont.

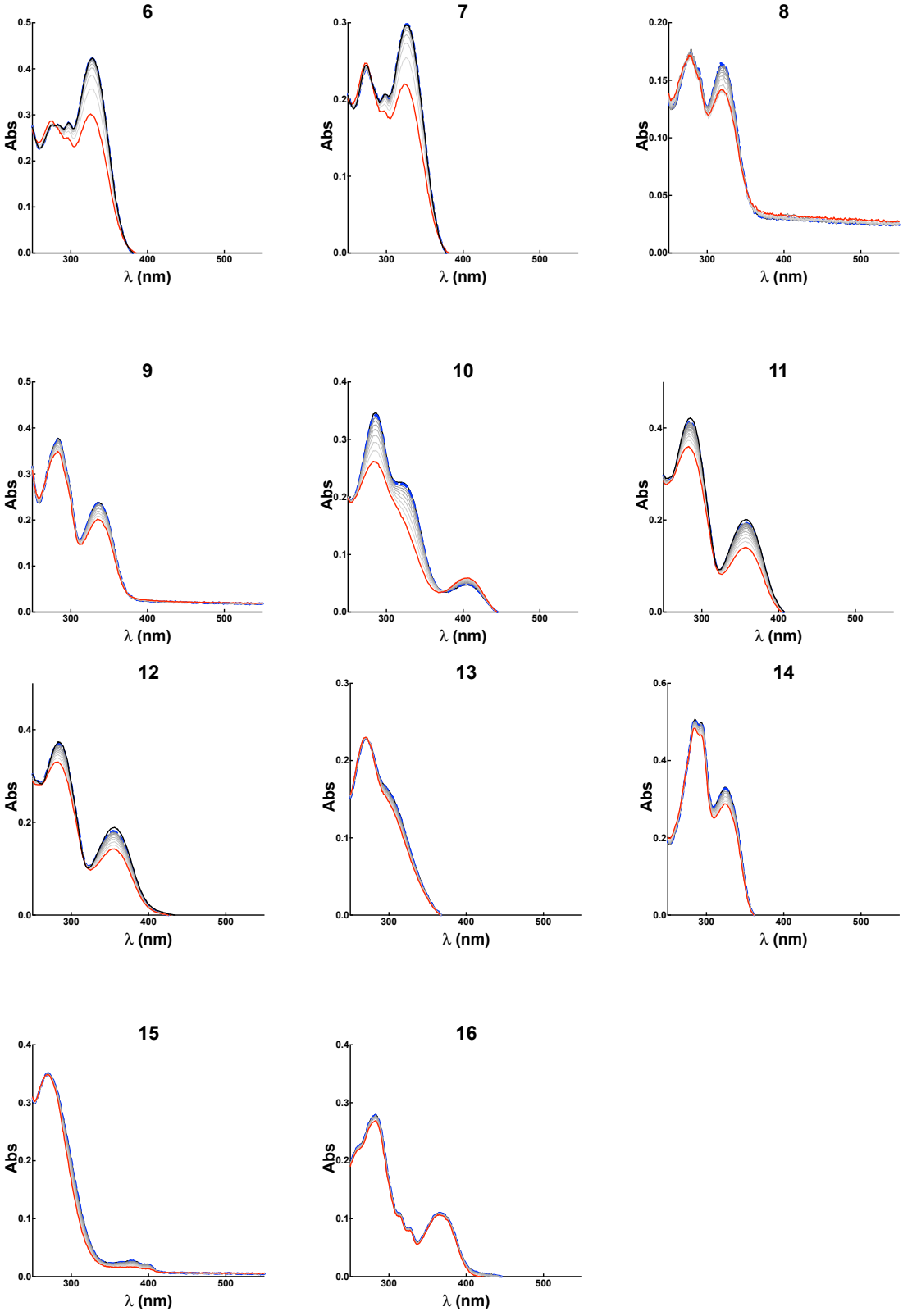

10. LC-MS of Initial and UVA/UVC PSS, calculating %conversion

LC-MS were taken on an Agilent 1200 System. Acquisition: Agilent 6224 TOF. 2 × 50 mm C-18 column, 2.5µm particle size, 220 µL s^{-1} flow rate. Organic solution B (3:100 Water:Acetonitrile) and aqueous solution A (100:3 Water:Acetonitrile) were mixed for the eluent. **B_0** signifies the initial percentage of solution B in the eluent, where **B_f** signifies the composition of maximum percentage of B reached at **T** minutes. The **B_0-B_f** transition was a linear change in the percent composition of the eluent. 20 µM solutions in acetonitrile were used with an injection volume of 4 µL. The UV peaks were studied at **Z** nm, the isosbestic point, to determine the relative populations of ground and photostationary states.

Compound	B_0 (%)	B_f (%)	T (min)	Z (nm)
HAPI	15	85	11	265
1	15	85	11	265
2	5	85	7	320
3	30	75	9	265
4	15	85	9	305
5	30	75	9	260
6	15	85	9	285
7	5	85	11	285
8	5	85	9	285
9	30	75	9	265
10	15	85	11	260
11	15	75	9	325
12	5	85	9	310
13	5	85	9	280
14	30	75	9	280
15	5	85	9	275
16	30	75	11	275

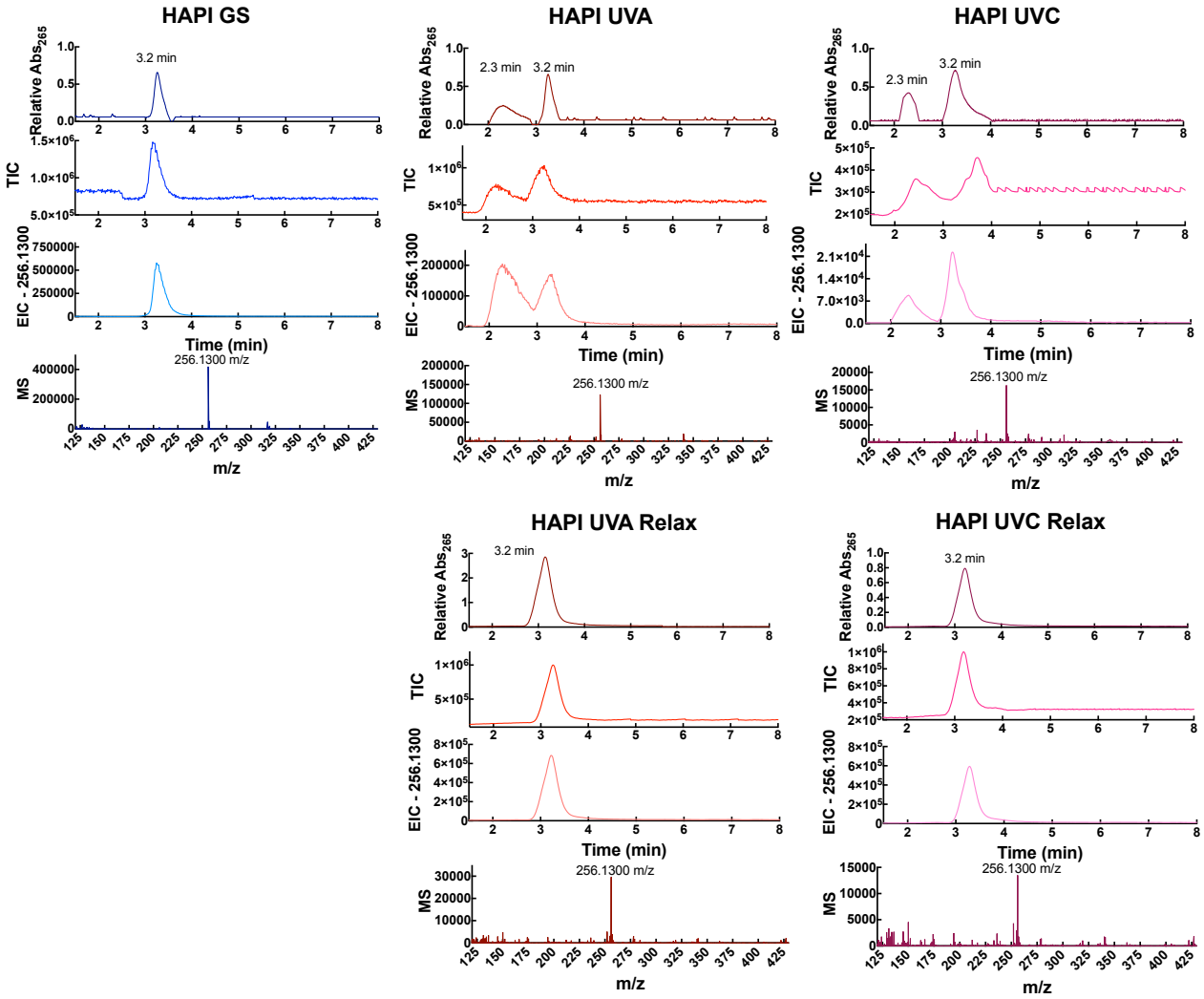

Figure S8. LC-MS characterization of HAPI. (**GS**): a 20-μM solution of HAPI in MeCN injected for LC-MS analysis shows only one peak eluting at 3.2 min, attributed to the *E* isomer. (**UVA/UVC**): a sample was then irradiated with either UVA or UVC light to its PSS, and was immediately injected for analysis. The additional peak eluting at 2.1 min with identical *m/z* value is attributed to the photoswitched *Z* isomer. (**UVA Relax/UVC Relax**)These irradiated samples were kept in the dark overnight, and injected for LC-MS analysis the next day. The solo peak at 3.2 min indicates a return to the ground state and demonstrates a reversible photoreaction.

Other Derivatives

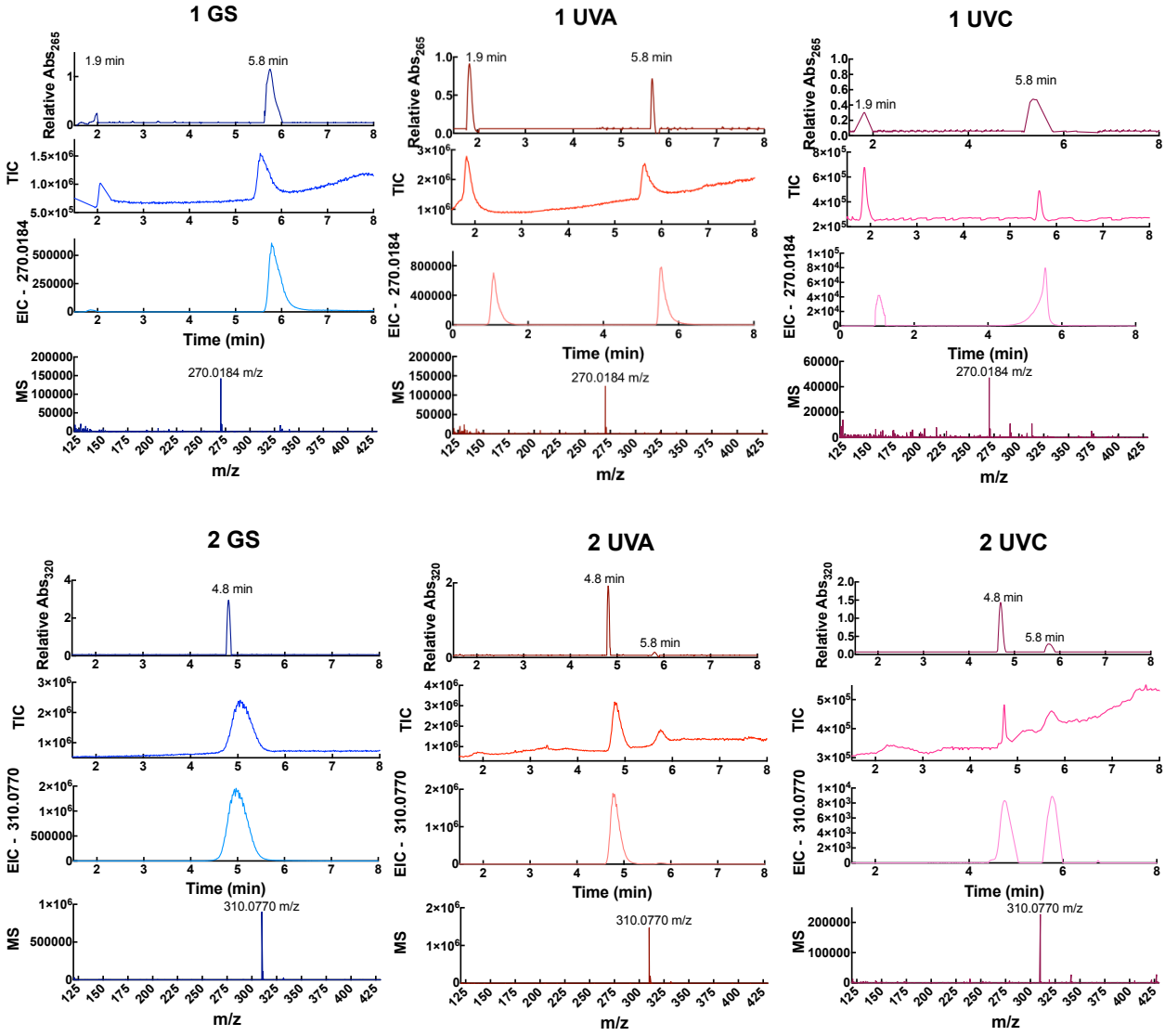

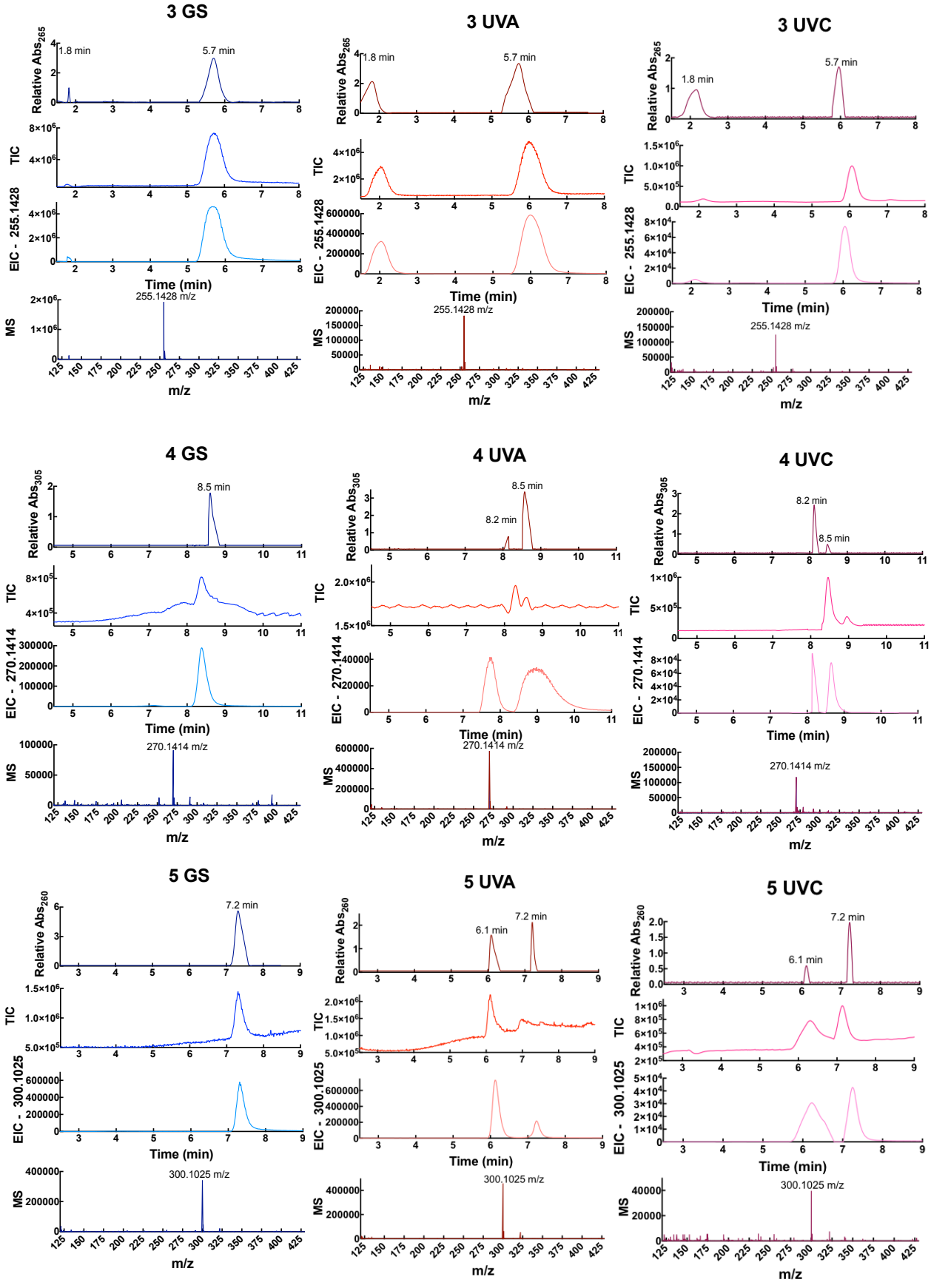
3 GS
3 UVA
3 UVC
4 GS
4 UVA
4 UVC
5 GS
5 UVA
5 UVC
Relative Abs265
Relative Abs305
Relative Abs260
1.8 min
5.7 min
8.5 min
8.2 min
7.2 min
6.1 min
TIC
EIC - 255.1428
EIC - 270.1414
EIC - 300.1025
Time (min)
MS
255.1428 m/z
270.1414 m/z
300.1025 m/z
m/z

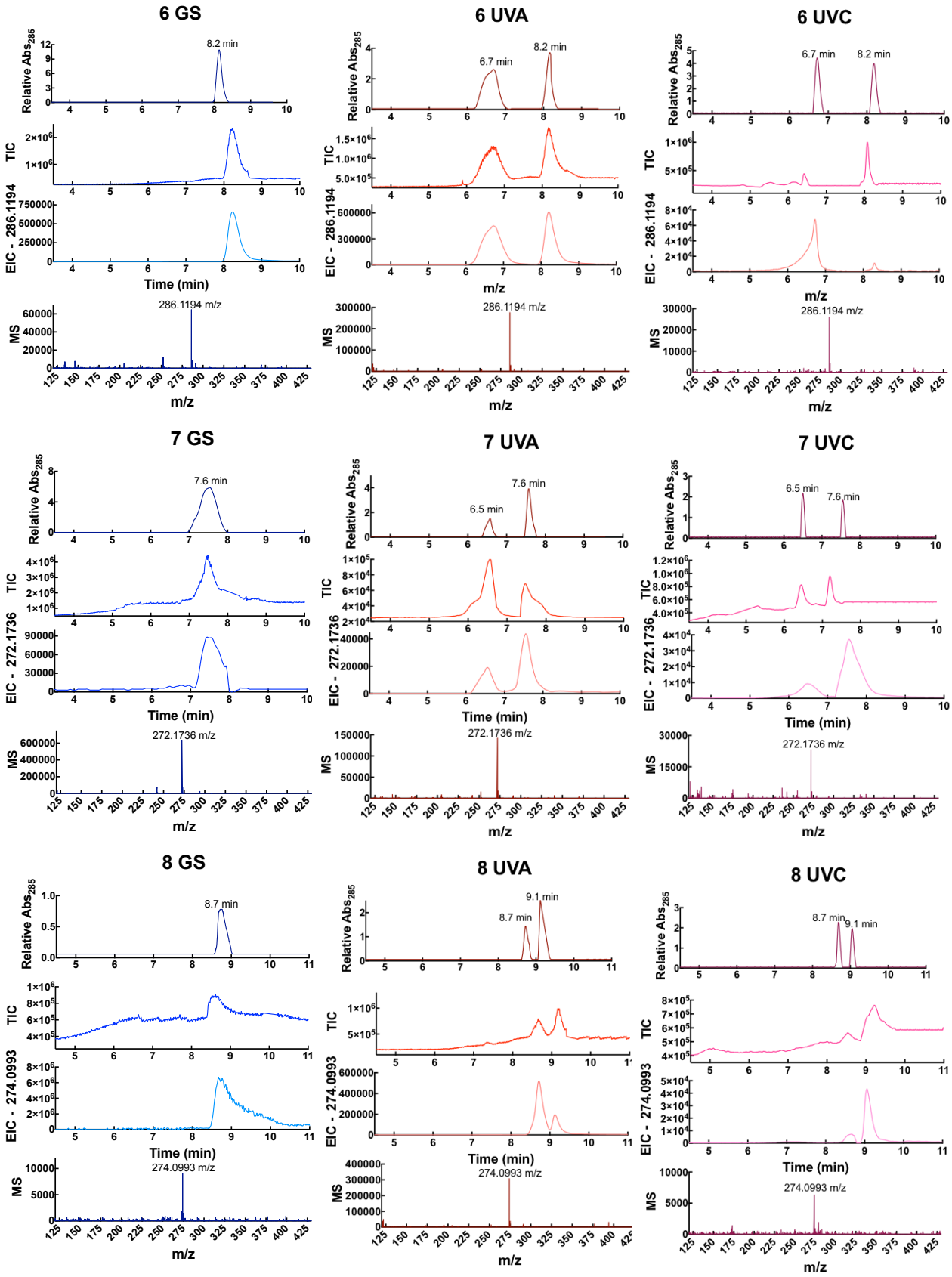
6 GS
6 UVA
6 UVC
7 GS
7 UVA
7 UVC
8 GS
8 UVA
8 UVC
Relative Abs285
TIC
EIC - 286.1194
EIC - 272.1736
EIC - 274.0993
MS
8.2 min
6.7 min
7.6 min
6.5 min
8.7 min
9.1 min
286.1194 m/z
272.1736 m/z
274.0993 m/z
Time (min)
m/z

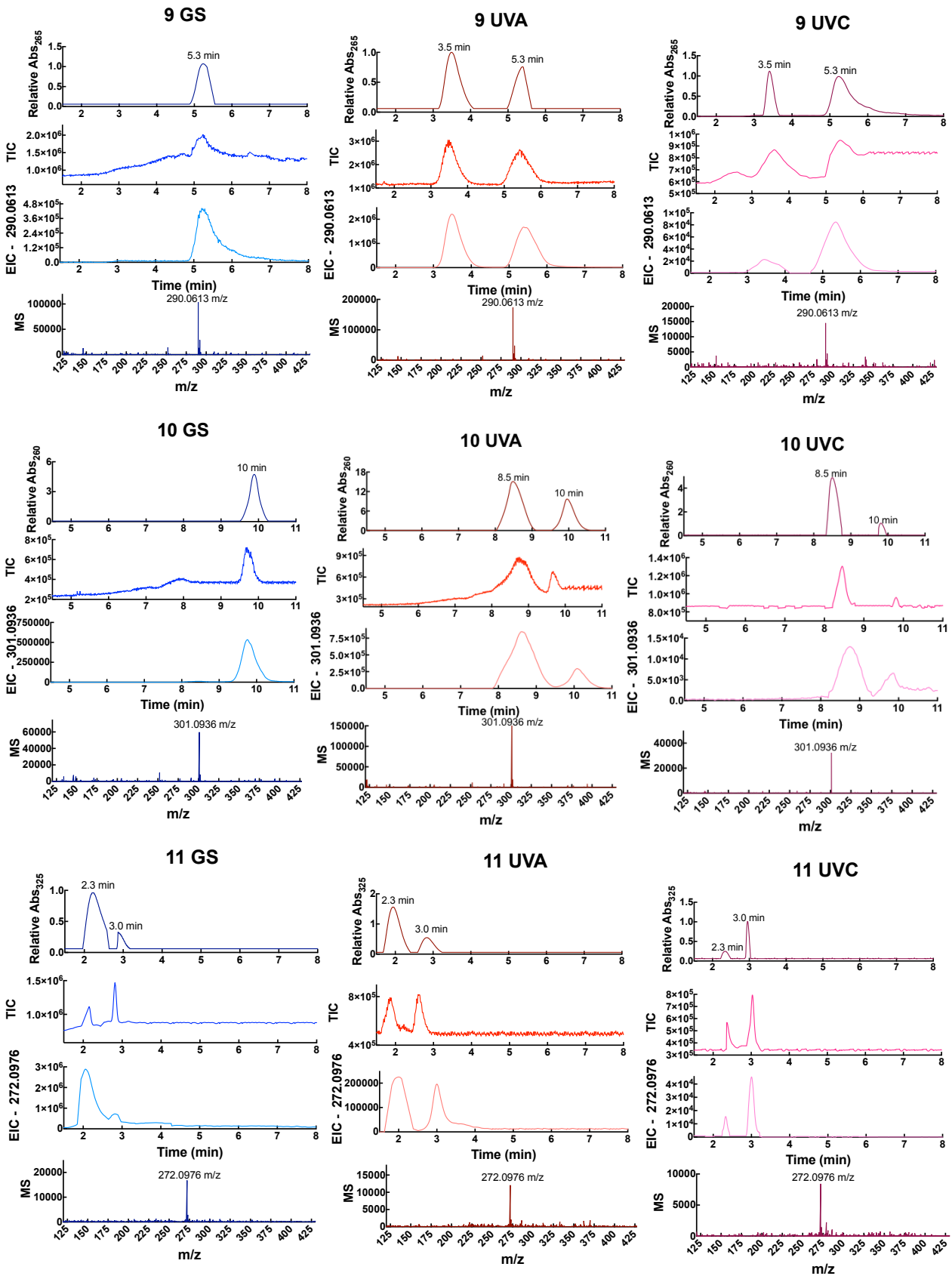
9 GS
9 UVA
9 UVC
10 GS
10 UVA
10 UVC
11 GS
11 UVA
11 UVC
Relative Abs265
Relative Abs260
Relative Abs325
TIC
EIC - 290.0613
EIC - 301.0936
EIC - 272.0976
MS
Time (min)
m/z
5.3 min
3.5 min
10 min
8.5 min
2.3 min
3.0 min
290.0613 m/z
301.0936 m/z
272.0976 m/z

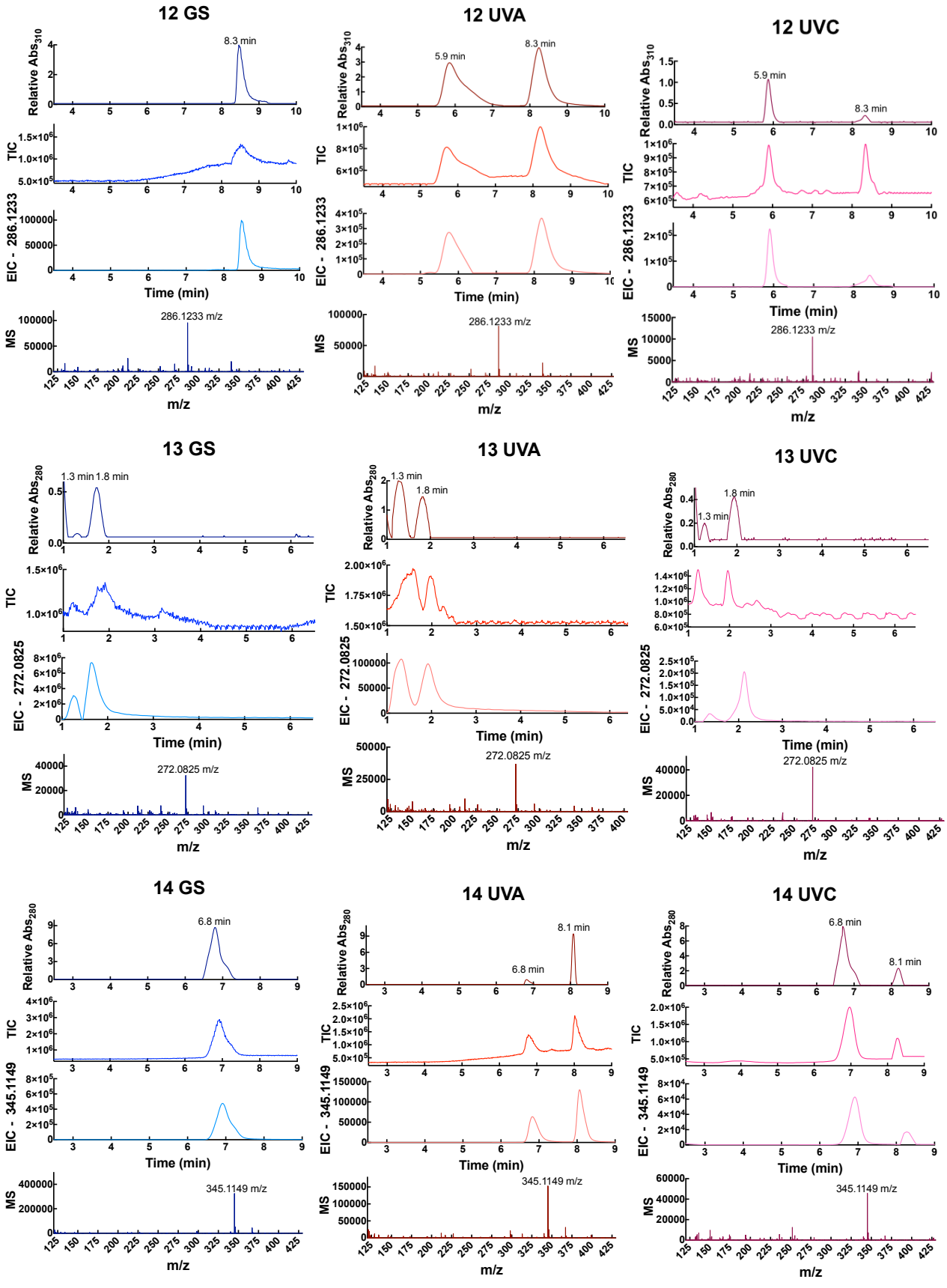
12 GS
12 UVA
12 UVC
Relative Abs310
TIC
EIC - 286.1233
MS
8.3 min
5.9 min
286.1233 m/z
Time (min)
m/z
13 GS
13 UVA
13 UVC
Relative Abs280
1.3 min
1.8 min
EIC - 272.0825
272.0825 m/z
14 GS
14 UVA
14 UVC
6.8 min
8.1 min
EIC - 345.1149
345.1149 m/z

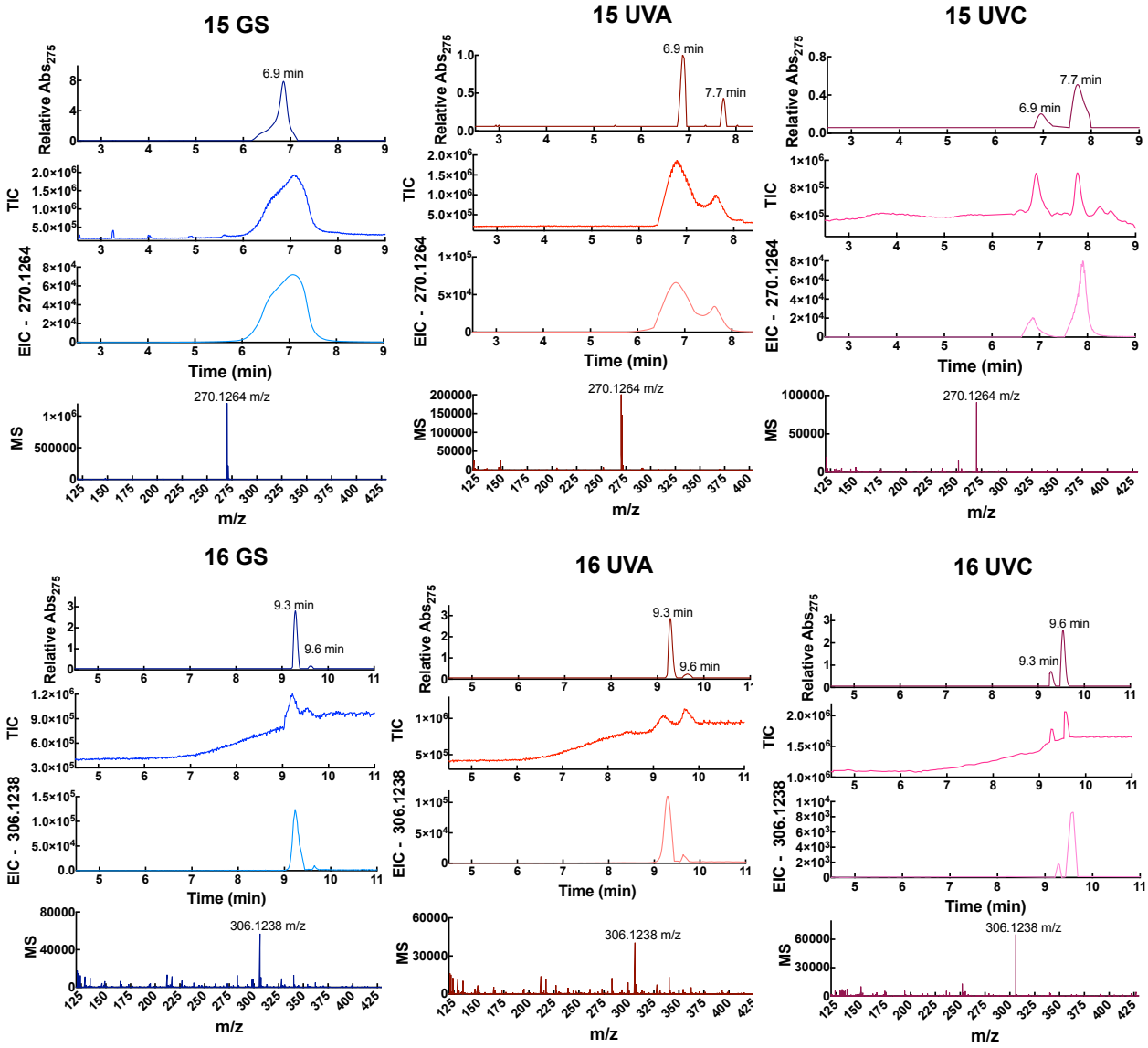

The Fraction of *E* in the ground state was calculated from the LC-MS data using the following equation:

$$\textit{Equation 1:} \qquad Fraction\ \mathrm{E}_{GS} = \frac{Area\ of\ \mathrm{E}_{GS}}{Area\ of\ \mathrm{E}_{GS} + Area\ \mathrm{Z}_{GS}}$$

The concentration of *E* in the ground state, $[E]_{GS}$ in μM, is calculated by:

$$\textit{Equation 2:} \qquad [E]_{GS} = Fraction\ \mathrm{E}_{GS} * [Total]_{GS}$$

The concentration of the two isomers at both the GS and UVA PSS is used further in calculations for molar absorptivity (see below).

The ratio of the two isomers are reported in **Table 1** of the main paper for ease of comparison. The ratio of E_{GS} is calculated by:

$$\textit{Equation 3:} \qquad Ratio\ E_{GS} = \frac{[E]_{GS}}{[E]_{GS} + [Z]_{GS}} * 100$$

These equations can be used to calculate Z_{GS}, E_{UVA}, Z_{UVA}, E_{UVC}, and Z_{UVC}.

11. Calculation of Extinctions Coefficients for *E* and *Z* isomers for HAPI & Derivatives

Determination of molar absorptivity for *E* and *Z* isomers

Absorbance spectrum of both the ground state and UVA-induced photostationary state was taken. Using the ratios of *E*/*Z* isomer found using LC-MS and absorbance of the two different states at a chosen wavelength, molar absorptivity for the *E* and *Z* isomer of each compound was calculated using the Beer-Lambert Law: $A=\varepsilon c l$.

Solving for ε_E

From the Beer-Lambert Law, we know that:

Equation 1 $$A_{\lambda max}^{GS} = \varepsilon_E c_E^{GS} + \varepsilon_Z c_Z^{GS}$$

Equation 2 $$A_{\lambda max}^{UVA} = \varepsilon_E c_E^{UVA} + \varepsilon_Z c_Z^{UVA}$$

where $A_{\lambda max}^{GS}$ is the absorbance at a specific wavelength in the ground state of the molecule, c_E^{GS} and c_Z^{GS} are the concentrations of the *E* and *Z* isomer in the ground state respectively, $A_{\lambda max}^{GS}$ is the absorbance at a specific wavelength in the photostationary state of the molecule, and c_E^{UVA} and c_Z^{UVA} are the concentrations of the *E* and *Z* isomer in the ground state respectively.

In *Equation 1*, we have two unknowns (ε_E and ε_Z). *Equation 2* can be rearranged to solve for ε_Z:

Equation 3 $$\varepsilon_Z = \frac{A_{\lambda max}^{UVA} - \varepsilon_E c_E^{UVA}}{c_Z^{UVA}}$$

Equation 3 can be substituted into *Equation 1*:

Equation 4 $$A_{\lambda max}^{GS} = \varepsilon_E c_E^{GS} + \left(\frac{A_{\lambda max}^{UVA} - \varepsilon_E c_E^{UVA}}{c_Z^{UVA}}\right) c_Z^{GS}$$

Equation 4 can be rearranged to solve for ε_E:

Equation 5 $$\varepsilon_E = \frac{A_{\lambda max}^{GS} - \left(\frac{A_{\lambda max}^{UVA} - c_Z^{GS}}{c_Z^{UVA}}\right)}{\left(\frac{c_E^{GS} - c_E^{UVA} c_Z^{GS}}{c_Z^{UVA}}\right)}$$

Once ε_E has been solved for, ε_Z can be solved for using *Equation 3*.

Table S2. Calculated extinction coefficients for both *E* and *Z* isomers calculated for each derivative at specified wavelength λ in DMSO.

	extinction coefficients in DMSO		
	λ	***e* ($M^{-1}cm^{-1}$)**	
	(nm)	***E***	***Z***
HAPI	331	10600	1800
1	331	10400	2000
2	310	5200	4000
3	329	15000	1100
4	333	28000	12200
5	338	21000	6600
6	333	19100	300
7	333	16000	2500
8	325	13500	2200
9	339	10200	2400
10	326	17200	12400
11	366	9100	1600
12	360	8200	15200
13	306	21200	2300
14	326	11800	100
15	286	11500	6300
16	366	15000	1500

12. Calculations for Composition of Blue Light Treatment

Since ε_Z and ε_E have been solved for, the composition of *E* and *Z* isomers after treatment with Blue light can be calculated.

We know that:

Equation 6 $$A_{\lambda max}^{BL} = \varepsilon_E c_E^{BL} + \varepsilon_Z c_Z^{BL}$$

Equation 7 $$C_{tot} = c_E^{BL} + c_Z^{BL}$$

Equation 7 can be rearranged to solve for c_Z^{BL}:

Equation 8 $$c_Z^{BL} = C_{tot} - c_E^{BL}$$

Equation 8 can be substituted into *Equation 6*:

Equation 9 $$A_{\lambda max}^{BL} = \varepsilon_E c_E^{BL} + \varepsilon_Z (C_{tot} - c_E^{BL})$$

Equation 9 can be rearranged to solve for c_E^{BL}:

Equation 10 $$c_E^{BL} = \frac{A_{\lambda max}^{BL} - \varepsilon_Z C_{tot}}{\varepsilon_E - \varepsilon_Z}$$

Once c_E^{BL} has been solved for, it can be substituted back into *Equation 7* to solve for c_Z^{BL}.

13. HAPI Thermal Relaxation Rates in Different Solvents

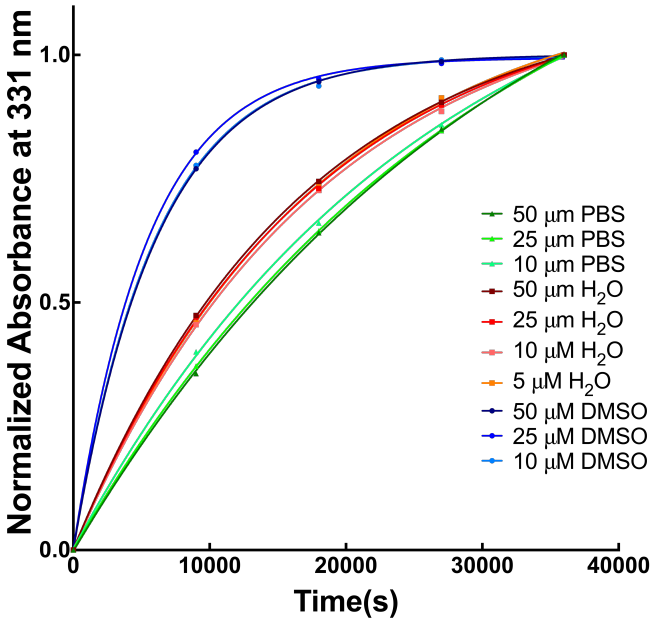

Figure S9. Thermal relaxation rates and half-lives of HAPI* in different solvent conditions after irradiation with UVA light. 3 concentrations were used to demonstrate an independence of the rate on concentration (4 for H_2O). At each concentration, the sample was irradiated with UVA light until the PSS was reached. Samples were monitored by UV-vis at 331 nm. Time-points were taken every 2.5 hours over a 10-hour period to monitor the thermal relaxation from *Z* to *E*. Data for each compound was normalized ($X-X_{min}/X_{max}-X_{min}$) and a non-linear regression one-phase association fit using Prism graphing software was applied to give the rate (*k*) and half-life. **Instrument settings:** Ave time – 0.0125 s.

PBS

	50 µm PBS	**25 µm PBS**	**10 µm PBS**	**Average**	**Standard Deviation**	**Percent Difference**
***k* (sec^{-1})**	0.000031	0.000033	0.000039	0.000034	0.000004	22
Half-life (sec)	22227	20855	17819	20300	2256	

H_2O

	50 µm H_2O	**25 µm H_2O**	**10 µM H_2O**	**5 µM H_2O**	**Average**	**Standard Deviation**	**Percent Difference**
***k* (sec^{-1})**	0.000060	0.000058	0.000055	0.000057	0.000057	0.000002	8.7
Half-time (sec)	11526	11969	12576	12198	12067	439	

DMSO

	50 µM DMSO	**25 µM DMSO**	**10 µM DMSO**	**Average**	**Standard Deviation**	**Percent Difference**
***k* (sec^{-1})**	0.00016	0.00018	0.00017	0.00017	0.00001	11
Half-life (sec)	4260	3800	4197	4086	249	

Percent difference was calculated between the fastest and slowest thermal relaxation rate within a specific solvent condition using the following equation:

$$Percent\ Difference = \frac{|x_1 - x_2|}{\frac{(x_1 + x_2)}{2}} * 100$$

14. Effect of sampling time of UV-vis on HAPI equilibrium

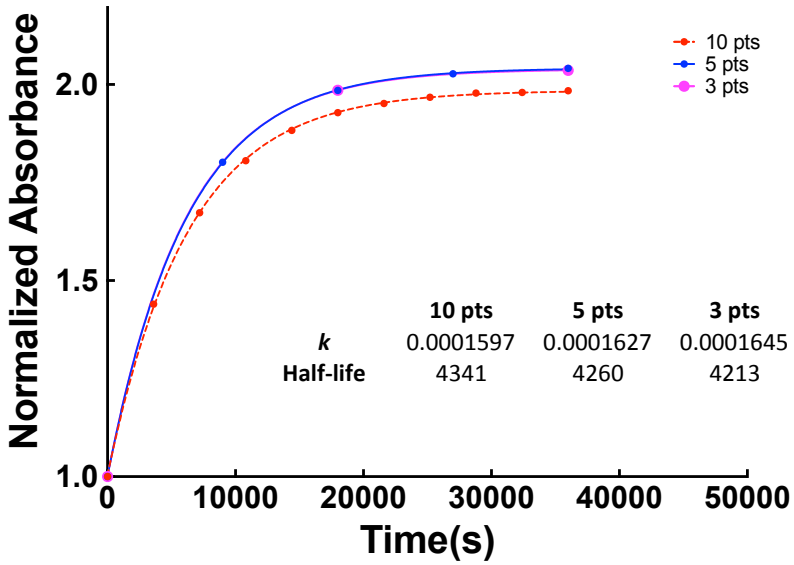

Figure S10. Effect of sampling time of UV-VIS on HAPI isomer equilibrium. Since HAPI and the derivatives are photoswtiches, it was important to ensure the sampling rate of the UV-vis was not affecting the equilibrium of the *E* and *Z* isomers. To ensure the method was satisfactory, the thermal relaxation rate of HAPI was measured for different sampling rates. Samples of 50 μM HAPI in DMSO were irradiated to the PSS with UVA light then monitored by UV-vis at 331 nm to watch the thermal relaxation from *Z* to *E*. Time points at different times over a 10-hour period, which allowed for different amounts of exposure to sampling light. Data for each compound were normalized ($X\text{-}X_{min}/X_{max}\text{-}X_{min}$) and a non-linear regression one-phase association fit using Prism graphing software was applied to give the rate (*k*) and half-life.

Instrument settings: Ave time – 0.0125 s; 10 pt. line – scanned every 3600 s; 5 pt. line – scanned every 9000 s; 3 pt. line – scanned every 12000 s.

Sampling the solution 10 times over the course of 10 hours had a slower thermal relaxation rate as compared to sampling 3 or 5 times, indicating sample rate can effect isomer equilibrium, Since sampling 3 and 5 times have rates that are within error, it was concluded that taking a scan 5 times over the course of 10 hours affected the equilibrium minimally while allowing better resolution of the data.

15. Assessment of Iron(III) Affinity

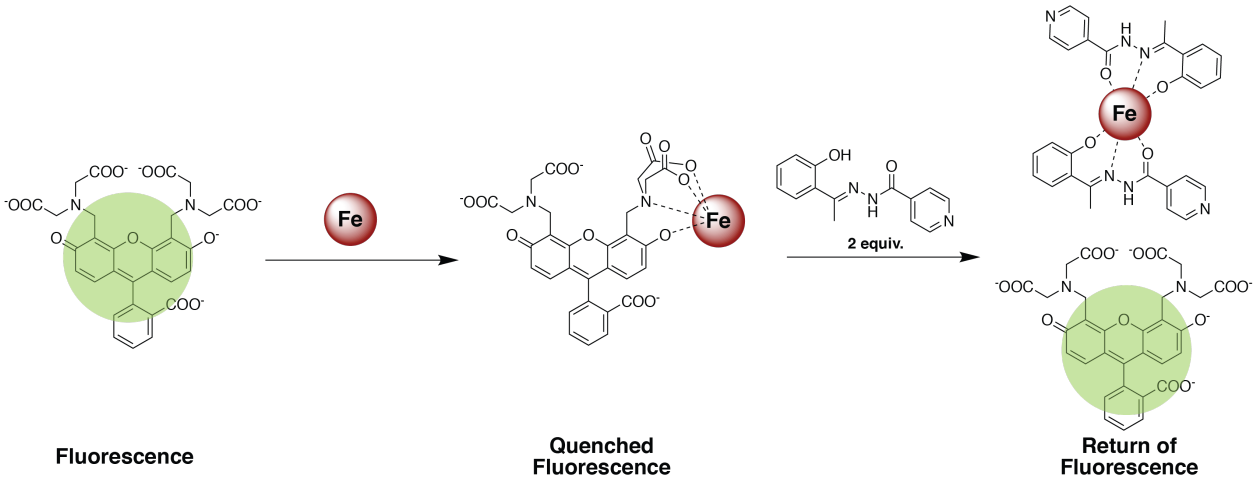

Figure S11. A competitive metal binding experiment was performed in a microwell plate between Fe(calcein) and chelating hydrazones (with or without prior UVA exposure). The fluorescence of calcein complexed with Fe^{3+} is quenched. Removal of Fe^{3+} from its complex with calcein restores calcein emission.

1. H. J. Kuhn, S. E. Braslavsky and R. Schmidt, *Pure Appl. Chem.*, 2004, **76**.
2. S. L. Murov, *Handbook of photochemistry [electronic resource]*, M. Dekker, New York, 1993.